

# Deep generative demixing: Recovering Lipschitz signals from noisy subgaussian mixtures

Aaron Berk<sup>1</sup>

<sup>1</sup>University of British Columbia  
Department of Mathematics  
1984 Mathematics Rd., Vancouver, BC, Canada V6T 1Z2

November 13, 2021

## Abstract

Generative neural networks (GNNs) have gained renown for efficaciously capturing intrinsic low-dimensional structure in natural images. Here, we investigate the subgaussian demixing problem for two Lipschitz signals, with GNN demixing as a special case. In demixing, one seeks identification of two signals given their sum and prior structural information. Here, we assume each signal lies in the range of a Lipschitz function, which includes many popular GNNs as a special case. We prove a sample complexity bound for nearly optimal recovery error that extends a recent result of Bora, *et al.* (2017) from the compressed sensing setting with gaussian matrices to demixing with subgaussian ones. Under a linear signal model in which the signals lie in convex sets, McCoy & Tropp (2014) have characterized the sample complexity for identification under subgaussian mixing. In the present setting, the signal structure need not be convex. For example, our result applies to a domain that is a non-convex union of convex cones. We support the efficacy of this demixing model with numerical simulations using trained GNNs, suggesting an algorithm that would be an interesting object of further theoretical study.

## 1 Introduction

Generative neural networks (GNNs) are neural networks that are capable of *generating* data from a learned distribution. Recently, GNNs have gained popularity for their performance on modelling spaces of natural images [5, 7, 6, 14, 25]. For example, variational autoencoders (VAEs) are composed of a “decoder” and “encoder” network, trained end-to-end to act as an approximate identity on the training distribution. The VAE learns a low-dimensional representation for elements within the data distribution [14] and its decoder is a type of GNN. For a thorough introduction to variational autoencoders, we recommend [5].

Recently, it was shown that some GNNs — including decoders from popular VAE architectures — could be used as structural proxies for generalized compressive sensing problems [1]. Roughly: it is possible to approximately recover a signal from a noisy underdetermined linear system with Gaussian measurements if the signal lies in the range of a Lipschitz function. The work specialized its recovery result from arbitrary Lipschitz functions, to the setting of Lipschitz-continuous neural networks. Many neural networks commonly used in practice are Lipschitz, supporting the relevance of this work to practical settings. For example, see [1, Lemma 4.2].

---

Several extensions of this work have been examined. In [30], the authors derive an improved sample complexity for compressed sensing-type problems when the underlying signal structure is the range of a ReLU neural network. Another version of this problem has been studied in which the measurements derive from a heavy-tailed, possibly corrupted distribution [11]. A further generalization studies the semi-parametrized single index model with possibly unknown possibly nonlinear link function, and in which the measurement vectors derive from a differentiable probability density function [30]. To our knowledge, a theoretical analysis of the *demixing problem* for two Lipschitz functions remains open.

The demixing problem refers to the identification of two unknown signals from their sum and given information about their structure. Sharp recovery bounds for *convex demixing problems* have been thoroughly investigated in [20], where the source signals are each assumed to be well encoded by some convex set. There, the authors show, under an *incoherence* condition, that recovery error depends on the *effective dimension* of the cones that govern the complexity of the source signals. Demixing with possibly unknown, possibly nonlinear link functions has been examined [27, 26]; however, the error bounds derived using this form of analysis may be coarse and difficult to analyze in practical settings [23].

The theory developed in [1] and [2] firmly lays the groundwork for the present work. Here, we investigate the demixing problem for two signals  $x^*, y^*$  that each lie in the range of an arbitrary Lipschitz function. We assume that  $x^*$  and  $y^*$  are combined by a *subgaussian random mixing operation* that we describe below, and seek approximate recovery of  $(x^*, y^*)$  *with high probability* on the mixing operation. The assumptions on the signal structure are mild, requiring only that each signal lie in the range of a Lipschitz function. These Lipschitz functions need not be the same, nor even have the same domain or range dimensions.

To specify, let  $G : \mathbb{R}^k \rightarrow \mathbb{R}^n$  and  $H : \mathbb{R}^{k'} \rightarrow \mathbb{R}^m$  be an  $L_G$ -Lipschitz and  $L_H$ -Lipschitz function. We will be concerned with the setting in which  $1 \leq k < n < \infty$  and  $1 \leq k' < m < \infty$ . We show that there are matrices  $A \in \mathbb{R}^{m \times n}$  such that, if  $x^* := G(u^*)$ ,  $y^* := H(v^*)$  for points  $(u^*, v^*) \in \mathbb{R}^k \times \mathbb{R}^{k'}$ , and

$$b = Ax^* + \sqrt{m}y^* + \eta \quad (1)$$

for some corruption  $\eta \in \mathbb{R}^m$ , then  $(x^*, y^*)$  may be approximated using only knowledge of  $(b, A, G, H)$ . Note the appearance of  $\sqrt{m}$  in (1) is for normalization purposes only, due to the definition of  $A$  below. The main result is stated in [Theorem 4](#).

A key tool in the proof of our results is a modified restricted isometry property (RIP), first presented in [1]. There, the authors proved the condition holds with high probability for matrices with normal random entries. Here, we show that the condition holds with high probability for an expanded class of matrices: namely, matrices  $A$  with independent isotropic subgaussian rows, as well as such concatenated matrices  $[I \ A]$ , where  $I$  is the identity matrix. Furthermore, we improve a result of [2] that establishes a deviation inequality for  $[I \ A]$ . We do this by improving the dependence on the subgaussian constant for  $A$  in the deviation inequality, using an improved Bernstein’s inequality first proved in [12]. This improvement is stated in [Theorem 6](#).

Finally, we support our theoretical results with numerical simulations presented in [Numerics](#). There, we use two trained VAEs to solve a noiseless demixing problem. We visualize the recovery performance of our proposed algorithm, and plot apparent exponential convergence of the objective function *vs.* iteration number. We include a discussion that highlights potential topics of further interest for empirical investigations.

**Motivation** The demixing problem can be viewed both as a tool for signal transmission, and as a tool for signal recovery. For example, the approach may be useful in the lossy transmission of two signals over a channel, where the sender and receiver possess the same Lipschitz continuous encoders  $G$  and  $H$ , and where the transmitted representation should use a small number of bits. In this scenario, the mixture may be amenable to further compression or encoding steps — such as that with error-correcting codes, or other sparsifying transforms [1, 19].

In [2], the expression (1) is used to describe the *corrupted sensing* model in which a ground truth signal  $x^*$ , after being encoded by  $A$ , is corrupted by (possibly unknown) structured noise  $y^*$ , and unknown, unstructured noise  $\eta$ . This interpretation translates to the present setting in the case where the structured noise process giving rise to  $y^*$  is well modelled by a Lipschitz function  $H$ . Of interest to the present setting would be the case where either  $H$  is a Lipschitz deep neural network that has been trained to model some noise process present in the corrupted measurements  $b$ .

## 2 Background

We start by introducing the set-restricted eigenvalue condition that is critical to the results developed in [1] and the present work. This condition is the “modified RIP” hinted at above.

**Definition** ([1, Definition 1]). Let  $S \subseteq \mathbb{R}^n$ . For some parameters  $\gamma > 0, \delta \geq 0$ , a matrix  $A \in \mathbb{R}^{m \times n}$  is said to satisfy the S-REC( $S, \gamma, \delta$ ) if  $\forall x_1, x_2 \in S$

$$\|A(x_1 - x_2)\| \geq \gamma \|x_1 - x_2\| - \delta.$$

Next, we include for reference the relevant result of [1], which uses S-REC for normal random matrices with iid entries to establish recovery bounds for compressed sensing (CS) with signals in the range of Lipschitz functions.

**Theorem** ([1, Theorem 1.2]). Let  $G : \mathbb{R}^k \rightarrow \mathbb{R}^n$  be an  $L$ -Lipschitz function. Let  $\Phi \in \mathbb{R}^{m \times N}$  be a random Gaussian matrix for  $m = \mathcal{O}\left(k \log \frac{Lr}{\delta}\right)$ , scaled so  $\Phi_{ij} \stackrel{iid}{\sim} \mathcal{N}(0, m^{-1})$ . For any  $x^* \in \mathbb{R}^N$  and any observation  $b = \Phi x^* + \eta$ , let  $\hat{u}$  minimize  $\|b - \Phi G(\cdot)\|_2$  to within additive  $\varepsilon$  of the optimum over vectors with  $\|\hat{u}\|_2 \leq r$ . Then, with probability  $1 - \exp(-\Omega(m))$ ,

$$\|G(\hat{u}) - x^*\|_2 \leq 6 \min_{\substack{u \in \mathbb{R}^k \\ \|u\|_2 \leq r}} \|G(u) - x^*\|_2 + 3\|\eta\|_2 + 2\varepsilon + 2\delta.$$

In extending [1, Theorem 1.2] to the demixing setting (cf. Theorem 4), we allow for a broader class of random matrices  $A$  appearing in (1). To define this class of matrices, we start by defining a subgaussian random variable and subgaussian random vector.

**Definition** (Subgaussian). For a random variable,  $X$ , say  $X$  is a *subgaussian random variable* with subgaussian norm bounded by  $K$ ,  $\|X\|_{\psi_2} \leq K$ , if for some  $K > 0$ ,

$$\mathbb{P}(|X| \geq t) \leq 2 \exp(-t^2/K^2), \quad \text{for all } t \geq 0.$$

For a random vector  $X' \in \mathbb{R}^n$ , say  $X$  is a *subgaussian random vector* with  $\|X'\|_{\psi_2} \leq K$  if

$$\sup_{e \in \mathbb{S}^{n-1}} \|\langle X, e \rangle\|_{\psi_2} \leq K.$$

Additionally, we say that two random vectors  $X, X' \in \mathbb{R}^n$  are *isotropic* if  $\mathbb{E} X' X^T = I_n$ .

**Definition** ( $K$ -subgaussian matrix). If  $A \in \mathbb{R}^{m \times n}$  is a matrix whose rows  $A_i \in \mathbb{R}^n$  are independent, isotropic subgaussian random vectors with norm at most  $K$ , we call  $A$  a  $K$ -subgaussian matrix.

Two geometric objects of particular importance to CS problems are the Gaussian width and Gaussian complexity, which often appear in deviation inequalities used to control  $K$ -subgaussian matrices on bounded sets.

**Definition** (Gaussian width/complexity). Define the Gaussian width  $w(\mathcal{T})$  and Gaussian complexity  $\gamma(\mathcal{T})$  of a set  $\mathcal{T} \subseteq \mathbb{R}^n$  by

$$w(\mathcal{T}) := \mathbb{E} \sup_{x \in \mathcal{T}} \langle x, g \rangle, \quad \gamma(\mathcal{T}) := \mathbb{E} \sup_{x \in \mathcal{T}} |\langle x, g \rangle|, \quad g_i \stackrel{\text{iid}}{\sim} \mathcal{N}(0, 1).$$

When  $A$  is a  $K$ -subgaussian matrix, we define  $B = B(A) := \begin{bmatrix} A & \sqrt{m}I \end{bmatrix}$  to be the concatenation of  $A$  with a scaled identity matrix (obtained by appending the columns of the second matrix to the first). We may alternately refer to  $B$  or  $A$  as the “subgaussian mixing matrix” or “mixing matrix”; it will be clear from context whether we mean  $B$  or  $A$ . To establish recovery bounds for the Lipschitz demixing problem with  $K$ -subgaussian matrices, we use an improved version of the following deviation inequality for subgaussian mixing matrices  $B$ .

**Theorem** ([2, Theorem 1]). *Let  $A \in \mathbb{R}^{m \times n}$  be a  $K$ -subgaussian matrix and  $\mathcal{T} \subseteq \mathbb{R}^n \times \mathbb{R}^m$  be bounded. Then*

$$\mathbb{E}_{(x,y) \in \mathcal{T}} \left| \|Ax + \sqrt{m}y\|_2 - \sqrt{m} \cdot \sqrt{\|x\|_2^2 + \|y\|_2^2} \right| \leq CK^2 \cdot \gamma(\mathcal{T})$$

For any  $t \geq 0$ , the event

$$\sup_{(x,y) \in \mathcal{T}} \left| \|Ax + \sqrt{m}y\|_2 - \sqrt{m} \cdot \sqrt{\|x\|_2^2 + \|y\|_2^2} \right| \leq CK^2 [\gamma(\mathcal{T}) + t \cdot \text{rad}(\mathcal{T})]$$

holds with probability at least  $1 - \exp(-t^2)$ .

Above,  $\text{rad}(\mathcal{T}) := \sup_{x \in \mathcal{T}} \|x\|_2$  denotes the radius of the set  $\mathcal{T}$ . Our improvement to this result, given in [Theorem 6](#), is to establish an improved dependence on the subgaussian constant  $K$ , from  $K^2$  to  $K\sqrt{\log K}$ .

Finally, we require [\[1, Lemma 4.3\]](#) to connect the aforementioned pieces. It is worth noting that this lemma essentially requires no modification from its original statement for it to be applicable to the demixing problem.

**Lemma** ([1, Lemma 4.3]). *Let  $A \in \mathbb{R}^{m \times n}$  be drawn from a distribution such that:*

1.  $\text{S-REC}(S, \gamma, \delta)$  holds with probability  $1 - p$ ;
2. for every fixed  $x \in \mathbb{R}^n$ ,  $\|Ax\|_2 \leq 2\|x\|_2$  with probability  $1 - p$ .

For any  $x^* \in \mathbb{R}^n$  and noise  $\eta \in \mathbb{R}^m$ , let  $y = Ax^* + \eta$ . Let  $\hat{x}$  satisfy

$$\|y - A\hat{x}\|_2 \leq \min_{x \in S} \|y - Ax\|_2 + \epsilon.$$

Then, with probability  $1 - 2p$ ,

$$\|\hat{x} - x^*\|_2 \leq \left( \frac{4}{\gamma} + 1 \right) \min_{x \in S} \|x^* - x\|_2 + \frac{1}{\gamma} (2\|\eta\|_2 + \epsilon + \delta).$$

As one final point regarding notation, we shall reserve the letters  $c, C > 0$  for absolute constants, whose value may change from one appearance to the next.

## 2.1 Two demixing modifications

Before moving on to the main results of this work, we discuss two modifications of the demixing problem (1), which trivially reduce to an application of [\[1, Theorem 1.2\]](#).

### 2.1.1 One mixing matrix

In the first modification, we assume that  $(x^*, y^*)$  are defined as in (1), and define instead  $b^{(1)} := \Phi(x^* + y^*) + \eta$ , where  $\Phi_{ij} \stackrel{\text{iid}}{\sim} \mathcal{N}(0, m^{-1})$  and  $\eta \in \mathbb{R}^m$  is some unknown fixed corruption. In this setting, we show that the two signals may be recovered but make no guarantee about correctly recovering each ground-truth signal.

For simplicity, assume  $k = k'$ ,  $L_G = L_H = L$  and define  $w^* := (u^*, v^*) \in \mathbb{R}^{2k}$ . Similarly, write  $w := (u, v) \in \mathbb{R}^{2k}$  and define the function  $F : \mathbb{R}^{2k} \rightarrow \mathbb{R}^n$  by  $F(w) := G(u) + H(v)$  so that  $b^{(1)} := \Phi F(w^*) + \eta \in \mathbb{R}^m$ . Using [1, Theorem 1.2], one may determine some  $\hat{w} \in \mathbb{R}^{2k}$  that approximates  $w^*$  with high probability on the matrix  $\Phi$ .

**Proposition 1.** *Suppose  $m \geq C \cdot 2k \log \left( \frac{2L\|w^*\|}{\delta} \right)$ . Let  $\hat{w} := (\hat{u}, \hat{v}) \in \mathbb{R}^{2k}$  minimize  $\|y - \Phi F(w)\|_2$  within additive error  $\varepsilon > 0$  over vectors  $w \in \mathbb{R}^{2k}$  with  $\|w\| \leq \|w^*\|$ . With probability at least  $1 - \exp(-cm)$ ,*

$$\|F(\hat{w}) - F(w^*)\|_2 = \|G(\hat{u}) - G(u^*) + H(\hat{v}) - H(v^*)\|_2 \leq 3\|\eta\|_2 + 2\varepsilon + 2\delta$$

*Proof.* The proof is a consequence of [1, Theorem 1.2]. Indeed, first notice that  $F$  is  $\sqrt{2}L$  Lipschitz, because  $G$  and  $H$  are  $L$ -Lipschitz:

$$\begin{aligned} \|F(w) - F(w')\|_2 &\leq \|G(u) - G(u')\| + \|H(v) - H(v')\| \leq L\|u - u'\| + L\|v - v'\| \\ &\leq \sqrt{2}L\sqrt{\|u - u'\|^2 + \|v - v'\|^2} = \sqrt{2}L\|w - w'\|_2. \end{aligned}$$

Next observe that  $F$  is a  $d$ -layer ReLU network because  $G$  and  $H$  are. Indeed, the linear transformations  $W_i^G \in \mathbb{R}^{k_i \times k_{i-1}}$ ,  $W_i^H \in \mathbb{R}^{k'_i \times k'_{i-1}}$  used in defining  $G$  and  $H$  can, at each layer, be merged into block-diagonal transformations

$$W_i := \begin{bmatrix} W_i^G & \mathbf{0} \\ \mathbf{0} & W_i^H \end{bmatrix} \in \mathbb{R}^{(k_i + k'_i) \times (k_{i-1} + k'_{i-1})}, i = 1, \dots, d.$$

to obtain

$$F(w) = [\text{Id}_n \text{Id}_n] \circ \sigma \circ W_d \circ \sigma \circ W_{d-1} \circ \dots \circ \sigma \circ W_1(w).$$

Applying [1, Theorem 1.2] thereby completes the proof.  $\square$

## 2.2 Two mixing matrices

Alternately, one may assume that  $x^*$  and  $y^*$  are mixed as  $b^{(2)} := \Phi_1 x^* + \Phi_2 y^* + \eta$ , where  $\Phi_i, i = 1, 2$  are independent and have the same distribution as  $\Phi$  above. Indeed, observe that  $b^{(2)}$  may be written as

$$b^{(2)} := \bar{\Phi} \begin{bmatrix} G(u^*) \\ H(v^*) \end{bmatrix} + \eta \quad \bar{\Phi} := \begin{bmatrix} \Phi_1 & \Phi_2 \end{bmatrix}.$$

Since the concatenated matrix  $\bar{\Phi}$  has entries  $\bar{\Phi}_{ij} \stackrel{\text{iid}}{\sim} \mathcal{N}(0, m^{-1})$ , a similar line of reasoning as in [One mixing matrix](#) using  $\bar{F}(w) := \begin{bmatrix} G(u) \\ H(v) \end{bmatrix}$  allows the approximate recovery  $\begin{bmatrix} \hat{x} \\ \hat{y} \end{bmatrix} \in \mathbb{R}^{2n}$  of  $\begin{bmatrix} x^* \\ y^* \end{bmatrix} \in \mathbb{R}^{2n}$  along with codes  $\hat{u}, \hat{v} \in \mathbb{R}^k$  with  $\hat{x} = G(\hat{u})$  and  $\hat{y} = H(\hat{v})$ .

We omit a formal proposition of this fact, noting that it would essentially be a re-wording of [1, Theorem 1.2].

### 3 Subgaussian Lipschitz demixing

Throughout this section, we assume the model (1), with  $A \in \mathbb{R}^{m \times n}$  being a  $K$ -subgaussian matrix. We further assume  $u^* \in B^k(r) \subseteq \mathbb{R}^k, v^* \in B^{k'}(r') \subseteq \mathbb{R}^{k'}$  for some  $r, r' > 0$ , with  $x^* := G(u^*)$  and  $y^* := H(v^*)$ . In particular, the model (1) becomes  $b^* := AG(u^*) + H(v^*) + \eta$  where  $\eta \in \mathbb{R}^m$ . Roughly, this section proves that if  $m$  is sufficiently large, then with high probability on the realization of  $A$ ,  $\hat{x} = G(\hat{u})$  and  $\hat{y} = H(\hat{v})$  may be obtained from  $(b, A, G, H)$  with  $\hat{x} \approx x^*$  and  $\hat{y} \approx y^*$ .

For notational brevity, we write  $\mathbb{B} := B^k(r) \times B^{k'}(r')$  and further write  $F(\mathbb{B}) := G(B^k(r)) \times H(B^{k'}(r'))$ . Finally, throughout this work we define  $\tilde{K} := K\sqrt{\log K}$ . As per the remark at the beginning of [12, §4.3], if  $X$  is a subgaussian random variable and  $\mathbb{E}|X|^2 = 1, \|X\|_{\psi_2} \leq K$ , then  $K \geq K_0 := (\log 2)^{-1/2} \approx 1.201$ . In particular, mandating isotropy of the rows implies  $1 < K \leq \tilde{K} \leq K^2$ .

The first lemma is a modification of [1, Lemma 8.2], adapted for the demixing problem. It establishes that mixing signals from  $F(\mathbb{B})$  is well approximated by mixing signals from a net for  $F(\mathbb{B})$ .

**Lemma 2.** Fix  $\delta > 0$ , define  $\kappa := m/n$  and suppose

$$m \geq Ck \log \left( \frac{crL_G\tilde{K}}{\delta} \right) + Ck' \log \left( \frac{cr'L_H\tilde{K}}{\delta} \right).$$

There is a net  $M \subseteq \mathbb{R}^k \times \mathbb{R}^{k'}$  for  $\mathbb{B} \subseteq \mathbb{R}^k \times \mathbb{R}^{k'}$  such that, for any  $z \in F(\mathbb{B})$ , if

$$z' \in \arg \min_{\hat{z} \in F(M)} \|z - \hat{z}\|_2$$

then  $m^{-1/2}\|B(z - z')\| \leq C\delta$  with probability at least  $1 - \exp(-cm)$ . Moreover, where  $C_\kappa > 0$  is an absolute constant depending only on  $\kappa$ , the cardinality of  $M$  satisfies

$$\log |M| \leq C_\kappa(k + k') + Ck \log \left( \frac{crL_G\tilde{K}}{\delta} \right) + Ck' \log \left( \frac{cr'L_H\tilde{K}}{\delta} \right).$$

Next, we establish that normalized subgaussian mixing matrices satisfy [1, Definition 1] with high probability.

**Lemma 3.** For  $\alpha < 1$ , if

$$m \geq \frac{C\tilde{K}^2}{\alpha^2} \left( k \log \left( \frac{L_G r}{\delta} \right) + k' \log \left( \frac{L_H r'}{\delta} \right) \right),$$

then  $m^{-1/2}B$  satisfies S-REC( $F(\mathbb{B}), 1 - \alpha, \delta$ ) with probability at least  $1 - \exp(-cm)$ .

The main result of this work follows by combining Lemma 2 and 3 with [1, Lemma 4.3].

**Theorem 4** (Lipschitz demixing). Fix  $\delta > 0$  and let  $A \in \mathbb{R}^{m \times n}$  be a  $K$ -subgaussian matrix. Suppose  $G : \mathbb{R}^k \rightarrow \mathbb{R}^n$  is  $L_G$ -Lipschitz,  $H : \mathbb{R}^{k'} \rightarrow \mathbb{R}^m$  is  $L_H$ -Lipschitz. Let  $z^* = [G(u^*)^T H(v^*)^T]^T$  for some  $(u^*, v^*) \in \mathbb{B}$ . Suppose  $b = Bz^* + \eta$  for some  $\eta \in \mathbb{R}^m$ . Suppose  $\hat{z} \in F(\mathbb{B}) := G(B^k(r)) \times H(B^{k'}(r'))$  satisfies  $\|B\hat{z} - b\|_2 \leq \min_{z \in F(\mathbb{B})} \|Bz - b\|_2 + \varepsilon$ . If

$$m \geq C\tilde{K}^2 \left( k \log \left( \frac{L_G r \tilde{K}}{\delta} \right) + k' \log \left( \frac{L_H r' \tilde{K}}{\delta} \right) \right),$$

then with probability at least  $1 - \exp(-cm)$  on the realization of  $A$ , it holds that

$$\|\hat{z} - z^*\| \leq C\tilde{K} \cdot \min_{z \in F(\mathbb{B})} \|z - z^*\| + C(2\|\eta\| + \delta + \varepsilon).$$

We defer the proofs of Lemma 2, 3 and Theorem 4 to Proofs for subgaussian Lipschitz demixing.

## 4 Improved subgaussian constant

Let  $A \in \mathbb{R}^{m \times n}$  be a  $K$ -subgaussian matrix. Where  $z = \begin{bmatrix} x \\ y \end{bmatrix} \in \mathbb{R}^n \times \mathbb{R}^m$ , define the centered random process  $X_z = X_{x,y}$  by

$$\begin{aligned} X_z &:= \|Ax + \sqrt{m}y\|_2 - (\mathbb{E} \|Ax + \sqrt{m}y\|_2^2)^{1/2} \\ &= \|Ax + \sqrt{m}y\|_2 - \sqrt{m} \cdot \sqrt{\|x\|_2^2 + \|y\|_2^2} \\ &= \|Bz\|_2 - \sqrt{m}\|z\|_2 \end{aligned} \tag{2}$$

That  $X_z$  is subgaussian (indeed, a process with subgaussian increments) was established by [2, Theorem 1]. In this section we improve the dependence of  $X_z$  on  $K$  from  $K^2$  to  $K\sqrt{\log K}$ . The tools required for this improvement were developed in [12].

**Lemma 5** (Improved subgaussian increments). *Let  $A \in \mathbb{R}^{m \times n}$  be a  $K$ -subgaussian matrix. The centered process  $X_z$  has subgaussian increments:*

$$\|X_z - X_{z'}\|_{\psi_2} \leq CK\sqrt{\log K}\|z - z'\|_2, \quad \text{for every } z, z' \in \mathbb{R}^n \times \mathbb{R}^m.$$

The proof of this result is technical, but strongly resembles the one presented in [2]. To prove Lemma 5 essentially requires replacing each application of Bernstein’s inequality in the proof of [2, Lemma 5] with one of [12, New Bernstein’s inequality]. We provide a detailed proof of Lemma 5 in Proofs for improved subgaussian constant.

Having established this result, it is straightforward to combine Lemma 5 with Talagrand’s majorizing measure theorem [29, Theorem 8.6.1] to obtain the desired improvement of [2, Theorem 1]. We relegate these technical details to Proofs for improved subgaussian constant.

**Theorem 6** (Improved deviation inequality). *Let  $A \in \mathbb{R}^{m \times n}$  be a  $K$ -subgaussian matrix and  $\mathcal{T} \subseteq \mathbb{R}^n \times \mathbb{R}^m$  be bounded. Then,*

$$\mathbb{E}_{(x,y) \in \mathcal{T}} \left| \|Ax + \sqrt{m}y\|_2 - \sqrt{m} \cdot \sqrt{\|x\|_2^2 + \|y\|_2^2} \right| \leq C\tilde{K} \cdot \gamma(\mathcal{T}).$$

Moreover, for any  $t \geq 0$ , the event

$$\sup_{(x,y) \in \mathcal{T}} \left| \|Ax + \sqrt{m}y\|_2 - \sqrt{m} \cdot \sqrt{\|x\|_2^2 + \|y\|_2^2} \right| \leq C\tilde{K}[\gamma(\mathcal{T}) + t \cdot \text{rad}(\mathcal{T})]$$

holds with probability at least  $1 - \exp(-t^2)$ .

## 5 Numerics

In this section we describe numerical results supporting the theory developed in Subgaussian Lipschitz demixing. We include only the main results of this simulation; specific implementation details beyond the general experimental set-up and simulation results may be found in Further Numerics Details.

For this simulation, two deep convolutional VAEs were trained on images of 1s and 8s, respectively; the trained decoders  $D_i : \mathbb{R}^{128} \rightarrow [0, 1]^{28 \times 28}$ ,  $i = 1, 8$  from each VAE were used as the Lipschitz-continuous deep generative

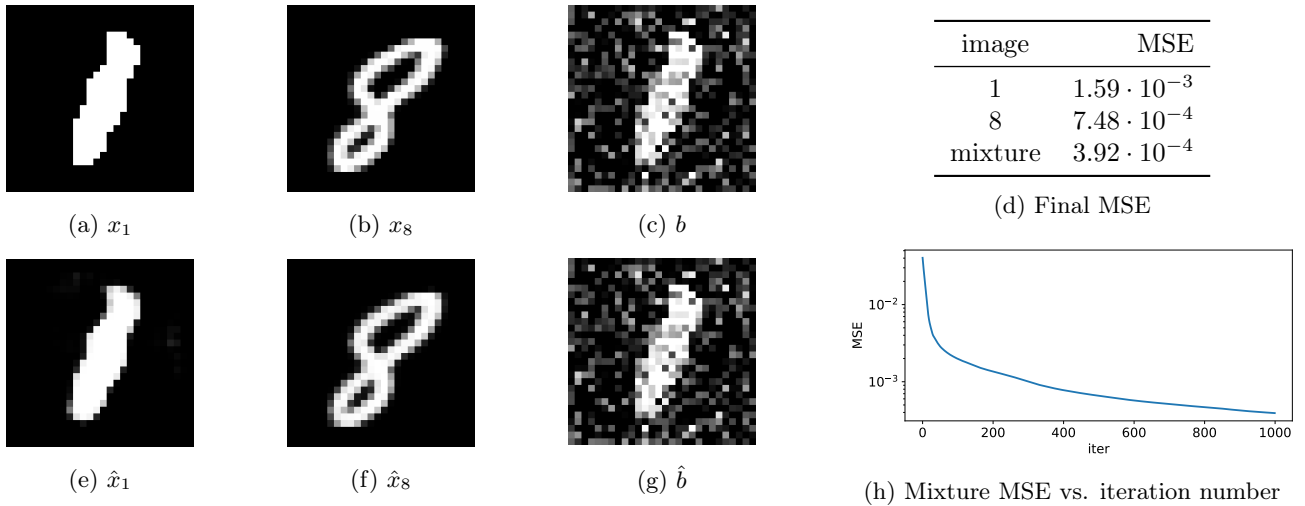


Figure 1: Demixing results for two deep generative networks. (a) & (b) Ground-truth images used to create (c) the mixture. (e) & (f) The recovered images are shown beside (g) the recovered mixture. (d) Final MSE for (e–g), resp. (h) A plot of mixture MSE *vs.* iteration number (log-y-scale)

networks for the demixing problem. A description of the network architecture and training method for the VAEs is detailed in [Further Numerics Details](#). We claim no novelty for our VAE or decoder architecture; extensions of VAEs involving convolutional layers appear in existing work [16, 24]. The digits used to train each VAE were a subclass of the MNIST database [3] containing only images of the digits 1 and 8. Each group of digits was randomly partitioned into training, validation and test sets. Only training and validation sets were used in the training of the VAEs.

Two ground-truth images (*cf.* [Figure 1a](#) & [1b](#), resp.) were randomly sampled from the test partition of each dataset and mixed according to (1), where the mixing matrix had iid normal random entries (*cf.* [Figure 1c](#)). In particular, where  $x_8 \in [0, 1]^{28 \times 28}$  is the (vectorized) grayscale image of an 8 and  $x_1 \in [0, 1]^{28 \times 28}$  that of a 1, the mixture is given by

$$b = \Phi x_8 + x_1, \quad \Phi \in \mathbb{R}^{784 \times 784}, \Phi_{ij} \stackrel{\text{iid}}{\sim} \mathcal{N}(0, \frac{1}{784}). \quad (3)$$

We did not investigate the effect of additive noise in this simulation, and leave that to a future work.

To solve the demixing problem, we used a variant of minibatch stochastic gradient descent [13] to minimize the mean-squared error (MSE) loss between the predicted mixture and the true mixture (using PyTorch [22]). Details for this numerical implementation, including pseudo-code, are provided in [Further Numerics Details](#). The recovered mixture is depicted in [Figure 1g](#), and the recovered signals, lying in the output of each generator  $D_i$ , are shown in [Figure 1e](#) and [1f](#) for  $i = 1, 8$ , respectively.

Convergence of the numerical implementation of the demixing algorithm is shown in [Figure 1h](#), where we plot the MSE loss between the true mixture and the predicted mixture as a function of the iteration number. The recovered image approximating  $x_1$  had an MSE of  $1.59 \cdot 10^{-3}$ ; that for  $x_8$ ,  $7.48 \cdot 10^{-4}$ ; and that for the mixture,  $3.92 \cdot 10^{-4}$ .



---

## 6 Conclusion

We prove a sample complexity bound for approximately solving the Lipschitz demixing problem with high probability on the subgaussian matrix  $A$ . This result extends existing work from CS with Lipschitz signals and Gaussian random matrices to the demixing problem with Lipschitz signals and  $K$ -subgaussian matrices. We establish an improved dependence on the subgaussian constant  $K$  appearing in the deviation inequality for subgaussian mixing matrices. We connect the demixing problem for Lipschitz signals to demixing for GNNs, noting that many popular GNNs are Lipschitz. To support the theory, we provide numerical simulations for demixing images of handwritten digits. Through these simulations we suggest a viable algorithm for demixing with trained GNNs, and demonstrate efficacy of the algorithm’s performance on a particular example.

Further analysis into the demixing of Lipschitz signals would be an interesting subject of future study — for instance, in the case where the mixing is not random, or where the networks remain untrained. For example, it would be of both theoretical and practical interest to analyze signal recovery in the setting where two signals each in the range of a GNN are mixed *without* the subgaussian mixing matrix:  $b = x^* + y^* + \eta$ . Here, establishing error bounds for approximate signal recovery may depend on the underlying geometric structure of the GNNs.

Additionally, theoretical analysis and thorough empirical exploration of our numerical algorithm remain open questions. For example, whether a convergence guarantee exists for the algorithm we have proposed, using GNNs, remains unknown. Further, we have chosen a particular initialization of the algorithm, but have not analyzed its effect on signal recovery in detail. A comparison of VAEs’ performance on the demixing problem using other datasets would be of interest, as would a comparison between VAEs and other GNNs such as GANs. Additionally, it could be worthwhile to validate numerically the effect of noise on demixing performance.

Finally, a further investigation may also wish to examine the case where the GNNs used as the Lipschitz functions  $G$  and  $H$  themselves have random weights. Such untrained networks have recently garnered attention as good structural priors for natural images [9, 10, 17], making them of potential interest to demixing.

## Acknowledgments

I would like to thank Drs. Babhru Joshi, Yaniv Plan, and Özgür Yilmaz for helpful discussion in the development and communication of this work.

## References

- [1] Ashish Bora, Ajil Jalal, Eric Price, and Alexandros G Dimakis. Compressed sensing using generative models. In *International Conference on Machine Learning*, pages 537–546, 2017.
- [2] Jinchu Chen and Yulong Liu. Stable recovery of structured signals from corrupted sub-gaussian measurements. *IEEE Transactions on Information Theory*, 65(5):2976–2994, 2018.
- [3] Li Deng. The MNIST database of handwritten digit images for machine learning research. *IEEE Signal Processing Magazine*, 29(6):141–142, 2012.
- [4] Sjoerd Dirksen. Tail bounds via generic chaining. *Electronic Journal of Probability*, 20, 2015.
- [5] Carl Doersch. Tutorial on variational autoencoders. *arXiv preprint arXiv:1606.05908*, 2016.

## REFERENCES

---

- [6] Ian Goodfellow. Tutorial: Generative adversarial networks. In *Proceedings of Neural Information Processing Systems*, 2016.
- [7] Ian Goodfellow, Jean Pouget-Abadie, Mehdi Mirza, Bing Xu, David Warde-Farley, Sherjil Ozair, Aaron Courville, and Yoshua Bengio. Generative adversarial nets. In *Advances in Neural Information Processing Systems*, pages 2672–2680, 2014.
- [8] Moritz Hardt, Ben Recht, and Yoram Singer. Train faster, generalize better: Stability of stochastic gradient descent. In *International Conference on Machine Learning*, pages 1225–1234, 2016.
- [9] R Heckel et al. Deep decoder: Concise image representations from untrained non-convolutional networks. In *International Conference on Learning Representations*, 2019.
- [10] Reinhard Heckel and Mahdi Soltanolkotabi. Compressive sensing with un-trained neural networks: Gradient descent finds the smoothest approximation. In *International Conference on Machine Learning*, 2020.
- [11] Ajil Jalal, Liu Liu, Alexandros G Dimakis, and Constantine Caramanis. Robust compressed sensing of generative models. *arXiv preprint arXiv:2006.09461*, 2020.
- [12] Halyun Jeong, Xiaowei Li, Yaniv Plan, and Özgür Yilmaz. Non-gaussian random matrices on sets: Optimal tail dependence and applications. In *2019 13th International conference on Sampling Theory and Applications (SampTA)*, pages 1–5. IEEE, 2019.
- [13] Diederik P Kingma and Jimmy Ba. Adam: A method for stochastic optimization. *arXiv preprint arXiv:1412.6980*, 2014.
- [14] Diederik P Kingma and Max Welling. Auto-encoding variational Bayes. *arXiv preprint arXiv:1312.6114*, 2013.
- [15] Diederik P Kingma and Max Welling. An introduction to variational autoencoders. *Foundations and Trends in Machine Learning*, pages 1–18, 2019. *arXiv preprint arXiv:1906.02691*.
- [16] Tejas D Kulkarni, William F Whitney, Pushmeet Kohli, and Josh Tenenbaum. Deep convolutional inverse graphics network. In *Advances in Neural Information Processing Systems*, pages 2539–2547, 2015.
- [17] Victor Lempitsky, Andrea Vedaldi, and Dmitry Ulyanov. Deep image prior. In *2018 IEEE/CVF Conference on Computer Vision and Pattern Recognition*, pages 9446–9454. IEEE, 2018.
- [18] Christopher Liaw, Abbas Mehrabian, Yaniv Plan, and Roman Vershynin. A simple tool for bounding the deviation of random matrices on geometric sets. In *Geometric aspects of functional analysis*, pages 277–299. Springer, 2017.
- [19] David JC MacKay. *Information theory, inference and learning algorithms*. Cambridge University Press, 2003.
- [20] Michael B McCoy and Joel A Tropp. Sharp recovery bounds for convex demixing, with applications. *Foundations of Computational Mathematics*, 14(3):503–567, 2014.
- [21] Stephen Odaibo. Tutorial: Deriving the standard variational autoencoder (vae) loss function. *arXiv preprint arXiv:1907.08956*, 2019.
- [22] Adam Paszke, Sam Gross, Soumith Chintala, Gregory Chanan, Edward Yang, Zachary DeVito, Zeming Lin, Alban Desmaison, Luca Antiga, and Adam Lerer. Automatic differentiation in PyTorch. In *NIPS Autodiff Workshop*, 2017.
- [23] Yaniv Plan and Roman Vershynin. The generalized Lasso with non-linear observations. *IEEE Transactions on Information Theory*, 62(3):1528–1537, 2016.

- 
- [24] Yunchen Pu, Zhe Gan, Ricardo Henao, Xin Yuan, Chunyuan Li, Andrew Stevens, and Lawrence Carin. Variational autoencoder for deep learning of images, labels and captions. In *Advances in Neural Information Processing Systems*, pages 2352–2360, 2016.
  - [25] Alec Radford, Luke Metz, and Soumith Chintala. Unsupervised representation learning with deep convolutional generative adversarial networks. *arXiv preprint arXiv:1511.06434*, 2015.
  - [26] Mohammadreza Soltani. *Provable algorithms for nonlinear models in machine learning and signal processing*. PhD thesis, Iowa State University, 2019.
  - [27] Mohammadreza Soltani and Chinmay Hegde. Demixing sparse signals from nonlinear observations. In *2016 50th Asilomar Conference on Signals, Systems and Computers*, 11 2016.
  - [28] Michel Talagrand. *The generic chaining: Upper and lower bounds for stochastic processes*. Springer, New York;Berlin;, 2005.
  - [29] Roman Vershynin. *High-dimensional probability: An introduction with applications in data science*, volume 47. Cambridge University Press, 2018.
  - [30] Xiaohan Wei, Zhuoran Yang, and Zhaoran Wang. On the statistical rate of nonlinear recovery in generative models with heavy-tailed data. In *International Conference on Machine Learning*, pages 6697–6706, 2019.

## A Proofs for §3

### A.1 Auxiliary results

**Proposition 7** (Gaussian complexity for  $|\mathcal{T}| = T$ ). *Assume that  $|\mathcal{T}| = T < \infty$ . Observe*

$$w(\mathcal{T}) \leq C\sqrt{\log T} \operatorname{diam}(\mathcal{T}); \quad \frac{1}{3} [w(\mathcal{T}) + \operatorname{rad}(\mathcal{T})] \leq \gamma(\mathcal{T}) \leq 2 \left[ w(\mathcal{T}) + \inf_{y \in \mathcal{T}} \|y\|_2 \right].$$

*Proof of Proposition 7.* The bound on  $w(\mathcal{T})$  follows from [29, Exercise 7.5.10], and the bounds on  $\gamma(\mathcal{T})$  follow from [29, Exercise 7.6.9].  $\square$

### A.2 Proof of Lemma 2

*Proof of Lemma 2.* Recall the definition of  $X_z$  in (2). Observe that for any fixed  $z \in \mathbb{R}^n \times \mathbb{R}^m$ ,  $X_z$  is a subgaussian random variable. For example, if  $z \in \mathbb{S}^{n+m-1}$ , it holds that

$$\mathbb{P} \left\{ |X_z| \geq C\tilde{K}t \right\} \leq \exp(-t^2).$$

Consequently, for any  $z \in \mathbb{R}^n \times \mathbb{R}^m$ ,

$$\mathbb{P} \left\{ \frac{|X_z|}{\sqrt{m}\|z\|_2} \geq C\tilde{K}t \right\} \leq \exp(-mt^2).$$

Substituting  $\varepsilon := Ct\tilde{K}$ , bounding the probability by a quantity  $f$  gives

$$\mathbb{P} \left\{ \frac{\|Bz\|_2}{\sqrt{m}} \geq (1 + \varepsilon)\|z\|_2 \right\} \leq \exp \left( -\frac{cm\varepsilon^2}{\tilde{K}^2} \right) = f, \quad \varepsilon = \sqrt{\frac{C\tilde{K}^2}{m} \log \left( \frac{1}{f} \right)}. \quad (4)$$

Next, our goal is to construct a chain of  $\delta_i$ -nets on  $F(\mathbb{B})$ . We do this by constructing a chain of nets on  $\mathbb{B}$ ,  $M := \{M_i\}_{i=0}^\ell$ , for which each net  $M_i$  will be a product of a net  $M_i^{(1)}$  on  $B^k(r)$  and  $M_i^{(2)}$  on  $B^{k'}(r')$ . In particular, for  $B^k(r), B^{k'}(r')$  [29, Corollary 4.2.13] gives the existence of  $\eta_i$ -nets  $M_i^{(1)}$  and  $\eta'_i$ -nets  $M_i^{(2)}$  respectively satisfying

$$\log |M_i^{(1)}| \leq k \log\left(1 + \frac{2r}{\eta_i}\right), \quad \log |M_i^{(2)}| \leq k' \log\left(1 + \frac{2r'}{\eta'_i}\right).$$

Choose:

$$\eta_i := \frac{\delta_i}{\sqrt{2}L_G}, \eta'_i := \frac{\delta_i}{\sqrt{2}L_H}, \quad \text{where } \delta_i := \delta_0/2^i, i \in [\ell],$$

and where  $\delta_0 > 0$  is any number satisfying  $\delta_0 < c\delta\tilde{K}^{-1}$  for some absolute constant  $c > 0$ . Then,

$$\begin{aligned} \log |M_i| &= \log |M_i^{(1)}| + \log |M_i^{(2)}| \leq k \log\left(\frac{2^i cr L_G}{\delta_0}\right) + k' \log\left(\frac{2^i cr' L_H}{\delta_0}\right) \\ &= i(k + k') \log 2 + k \log\left(\frac{cr L_G}{\delta_0}\right) + k' \log\left(\frac{cr' L_H}{\delta_0}\right) \end{aligned}$$

Observe that  $N_i := F(M_i)$  is a  $\delta_i$ -net for  $F(\mathbb{B})$ : for any  $(u, v) \in \mathbb{B}$  there exists  $(u', v') \in M_i$  with

$$\begin{aligned} \|F(u, v) - F(u', v')\|_2 &= \sqrt{\|G(u) - G(u')\|_2^2 + \|H(v) - H(v')\|_2^2} \\ &\leq \sqrt{L_G^2 \|u - u'\|_2^2 + L_H \|v - v'\|_2^2} \leq \delta_i \end{aligned}$$

Next, define

$$T_i := \{z_{i+1} - z_i : z_{i+1} \in N_{i+1}, z_i \in N_i\}$$

and observe that  $T_i$  has cardinality satisfying

$$\begin{aligned} \log |T_i| &\leq \log(|N_{i+1}| |N_i|) \leq \log(|M_{i+1}| |M_i|) \\ &\leq C(2i + 1)(k + k') + 2k \log\left(\frac{cr L_G}{\delta_0}\right) + 2k' \log\left(\frac{cr' L_H}{\delta_0}\right). \end{aligned}$$

Eventually, for a collection  $(\varepsilon_i, f_i)$  connected as in (4), we will union bound to obtain

$$\mathbb{P}\left\{\frac{\|B\zeta\|}{\sqrt{m}} \leq (1 + \varepsilon_i)\|\zeta\|, \forall i, \forall \zeta \in T_i\right\} \geq 1 - \sum_{i=0}^{\ell-1} |T_i| f_i. \quad (5)$$

We start by ensuring the right-hand side of the above expression is small. Using

$$\begin{aligned} \log(|T_i| f_i) &= \log |T_i| + \log(f_i) \\ &\leq C(2i + 1)(k + k') + 2k \log\left(\frac{cr L_G}{\delta_0}\right) + 2k' \log\left(\frac{cr' L_H}{\delta_0}\right) + \log(f_i), \end{aligned} \quad (6)$$

and choosing

$$m \geq 2k \log\left(\frac{cr L_G}{\delta_0}\right) + 2k' \log\left(\frac{cr' L_H}{\delta_0}\right), \quad \log(f_i) = -\left(\frac{4m}{3} + C(3i + 1)(k + k')\right),$$

gives

$$\log(|T_i|f_i) \leq -Ci(k+k') - \frac{m}{3}.$$

In particular,

$$\sum_{i=0}^{\ell-1} |T_i|f_i \leq \exp\left(-\frac{m}{3}\right) \sum_{i=0}^{\ell-1} \exp(-Ci(k+k')) \leq \exp\left(-\frac{m}{3}\right) \frac{1}{1-e^{-C}} \leq C \exp\left(-\frac{m}{3}\right).$$

With the present choices, the expression for  $\varepsilon_i$  becomes, using [\(4\)](#),

$$\varepsilon_i = \sqrt{\frac{C\tilde{K}^2}{m} \log\left(\frac{1}{f_i}\right)} = C\tilde{K} \sqrt{1 + \frac{(3i+1)(k+k')}{m}}.$$

Now for any  $z \in F(\mathbb{B})$ , we can write

$$z = z_0 + (z_1 - z_0) + \cdots + (z_\ell - z_{\ell-1}) + z^f$$

where  $z_i \in N_i$ ,  $z^f := z - z_\ell$ . Using [\(5\)](#), since  $\zeta_i = z_{i+1} - z_i \in T_i$ , it holds with probability at least  $1 - C \exp(-m/3)$  that

$$\begin{aligned} m^{-1/2} \sum_{i=0}^{\ell-1} \|B\zeta_i\|_2 &\leq \sum_{i=0}^{\ell-1} (1 + \varepsilon_i) \|\zeta_i\|_2 \leq \delta_0 \sum_{i=0}^{\ell-1} 2^{-i} (1 + \varepsilon_i) \\ &\leq \delta_0 \sum_{i=0}^{\ell-1} 2^{-i} \left( 1 + C\tilde{K} \sqrt{1 + \frac{(3i+1)(k+k')}{m}} \right) \\ &\leq C\delta_0 \tilde{K} \sum_{i=0}^{\ell-1} \frac{1 + \sqrt{3i+1}}{2^i} \leq C\delta_0 \tilde{K} < \frac{\delta}{2}. \end{aligned}$$

Also observe that  $\|z^f\|_2 \leq \delta_0/2^\ell$  by construction.

Now, using [Theorem 6](#) with  $\mathcal{T} := \mathbb{S}^{n+m-1}$  we have

$$\sup_{z \in \mathcal{T}} \left| \frac{\|Bz\|_2}{\sqrt{m}} - 1 \right| \leq C\tilde{K} \left[ \sqrt{\frac{n+m}{m}} + 1 \right]$$

with probability at least  $1 - \exp(-m)$ . In particular, with the stated probability,

$$\left\| \frac{B}{\sqrt{m}} \right\| \leq C\tilde{K} \left( 2 + \sqrt{\frac{n+m}{m}} \right).$$

Therefore, with probability at least  $1 - \exp(-m)$  we have

$$m^{-1/2} \|Bz^f\|_2 \leq C\delta_0 \tilde{K} 2^{-\ell} \left( 2 + \sqrt{\frac{n+m}{m}} \right) \leq C\delta_0 \tilde{K} < \frac{\delta}{2},$$

achieved by taking  $\ell \geq C \log(2 + \kappa^{-1})$  where  $\kappa := m/n$  is the aspect ratio of  $A$ .

Combining the above results, and noting that it is possible to choose  $z' = z_0$ , it holds with probability at least  $1 - \exp(-cm)$  that

$$m^{-1/2} \|B(z - z')\|_2 = m^{-1/2} \|B(z - z_0)\|_2 \leq m^{-1/2} \|Bz^f\|_2 + m^{-1/2} \sum_{i=0}^{\ell-1} \|B\zeta_i\|_2 < \delta.$$

□

### A.3 Proof of Lemma 3

*Proof of Lemma 3.* Observe that there exists a net  $M := M^{(1)} \times M^{(2)}$  for  $\mathbb{B}$  where  $M^{(1)}$  is a  $\frac{\delta}{\sqrt{2}L_G}$ -net for  $B^k(r)$  and  $M^{(2)}$  is a  $\frac{\delta}{\sqrt{2}L_H}$ -net for  $B^{k'}(r')$ , with

$$\log |M| \leq \log |M^{(1)}| + \log |M^{(2)}| \leq k \log \left( 1 + \frac{2\sqrt{2}L_G r}{\delta} \right) + k' \log \left( 1 + \frac{2\sqrt{2}L_H r'}{\delta} \right).$$

By construction,  $F(M) = \{(G(u), H(v)) : (u, v) \in M\}$  is a  $\delta$ -net for  $F(\mathbb{B})$ . In particular, for any  $z, z' \in F(\mathbb{B})$  there are  $z_1, z_2 \in F(M)$  such that

$$\|z - z'\|_2 \leq \|z - z_1\|_2 + \|z_1 - z_2\|_2 + \|z_2 - z'\|_2 \leq \|z_1 - z_2\|_2 + 2\delta. \quad (7)$$

Moreover, for these points, applying Lemma 2 for a possibly larger net  $M$  gives

$$\|B(z_1 - z_2)\|_2 \leq \|B(z_1 - z)\|_2 + \|B(z - z')\|_2 + \|B(z' - z_2)\|_2 \leq \|B(z - z')\|_2 + C\delta\sqrt{m}. \quad (8)$$

Next, defining

$$\mathcal{T} := \left\{ \frac{z_1 - z_2}{\|z_1 - z_2\|_2} : z_1, z_2 \in F(M) \right\},$$

and noting  $\gamma(\mathcal{T}) \leq C\sqrt{\log |M|}$  by Proposition 7, we may use Lemma 5 to obtain

$$\sup_{z_1, z_2 \in F(M)} \left| \frac{\|B(z_1 - z_2)\|_2}{\sqrt{m}\|z_1 - z_2\|_2} - 1 \right| \leq C\tilde{K}\sqrt{\frac{\log |M|}{m}},$$

with probability at least  $1 - \exp(-m)$ . Accordingly, one has

$$(1 - \alpha)\|z_1 - z_2\|_2 \leq m^{-1/2}\|B(z_1 - z_2)\|_2 \leq (1 + \alpha)\|z_1 - z_2\|_2 \quad (9)$$

with probability at least  $1 - \exp(-m)$  provided that

$$m \geq \frac{C\tilde{K}^2}{\alpha^2}(k + k') \log \left( \frac{\lambda\tilde{K}}{\delta} \right) \geq \frac{C\tilde{K}^2}{\alpha^2} \log |M|, \quad \lambda := \max\{L_G r, L_H r'\}. \quad (10)$$

Combining (7–9) under condition (10) gives, for any  $z, z' \in F(\mathbb{B})$ ,

$$\begin{aligned} (1 - \alpha)\|z - z'\|_2 &\leq (1 - \alpha)\|z_1 - z_2\|_2 + 2\delta \leq \|m^{-1/2}B(z_1 - z_2)\|_2 + 2\delta \\ &\leq \|m^{-1/2}B(z - z')\|_2 + 4\delta. \end{aligned}$$

with probability at least  $1 - \exp(-cm)$ .

□

*Remark 1* (Simplified sample complexity bound). The expression appearing in (10),

$$m \geq \frac{C\tilde{K}^2}{\alpha^2}(k + k') \log \left( \frac{\lambda\tilde{K}}{\delta} \right),$$

is simpler (*i.e.*, more aesthetic) than the analogous condition appearing in the statement of Lemma 3, but also a stronger assumption on  $m$ , due to the definition of  $\lambda$ .

## A.4 Proof of Theorem 4

Before proving Theorem 4, we modify [1, Lemma 4.3] so that the statement fits the present setting.

**Lemma 8** (modified [1, Lemma 4.3]). *Let  $\tilde{B} := \begin{bmatrix} \tilde{A} & I_m \end{bmatrix}$  where  $\tilde{A} \in \mathbb{R}^{m \times n}$  is drawn from a distribution such that:*

1.  $\tilde{B}$  satisfies S-REC( $S, \gamma, \delta$ ) with probability  $1 - p$ ;
2.  $\|\tilde{B}z\|_2 \leq C\tilde{K}\|z\|_2$  for every fixed  $z \in \mathbb{R}^n \times \mathbb{R}^m$  with probability  $1 - p$ .

For any  $z^* \in \mathbb{R}^n \times \mathbb{R}^m$  and noise  $\eta \in \mathbb{R}^m$ , let  $b = \tilde{B}z^* + \eta$ . Let  $\hat{z}$  satisfy

$$\|b - \tilde{B}\hat{z}\|_2 \leq \min_{z \in S} \|b - \tilde{B}z\|_2 + \epsilon.$$

Then, with probability  $1 - 2p$ ,

$$\|\hat{z} - z^*\|_2 \leq \left( \frac{C\tilde{K}}{\gamma} + 1 \right) \min_{z \in S} \|z^* - z\|_2 + \frac{1}{\gamma} (2\|\eta\|_2 + \epsilon + \delta).$$

*Proof of Lemma 8.* We proceed as in the proof of [1, Lemma 4.3]. Define  $\bar{z} \in \arg \min_{z \in S} \|z^* - z\|_2$ . Since  $\tilde{B}$  satisfies S-REC( $S, \gamma, \delta$ ), with probability  $1 - p$ , it holds with probability  $1 - p$ , using the assumption on  $\hat{z}$ , that

$$\begin{aligned} \|\bar{z} - \hat{z}\|_2 &\leq \gamma^{-1} \left( \|\tilde{B}\bar{z} - b\|_2 + \|\tilde{B}\hat{z} - b\|_2 + \delta \right) \leq \gamma^{-1} \left( \|\tilde{B}\bar{z} - b\|_2 + \min_{z \in S} \|\tilde{B}z - b\|_2 + \delta + \epsilon \right) \\ &\leq \gamma^{-1} \left( 2\|\tilde{B}\bar{z} - b\|_2 + \delta + \epsilon \right) \leq \gamma^{-1} \left( 2\|\tilde{B}(\bar{z} - z^*)\|_2 + \delta + \epsilon + 2\|\eta\|_2 \right) \end{aligned}$$

By assumption, it also holds with probability at least  $1 - p$  that  $\|\tilde{B}(\bar{z} - z^*)\|_2 \leq C\tilde{K}\|\bar{z} - z^*\|_2$ . Therefore, with probability at least  $1 - 2p$ ,

$$\begin{aligned} \|z^* - \hat{z}\|_2 &\leq \|z^* - \bar{z}\|_2 + \|\bar{z} - \hat{z}\|_2 \\ &\leq \|z^* - \bar{z}\|_2 + \gamma^{-1} \left( 2\|\tilde{B}(\bar{z} - z^*)\|_2 + \delta + \epsilon + 2\|\eta\|_2 \right) \\ &\leq \|z^* - \bar{z}\|_2 + \gamma^{-1} \left( C\tilde{K}\|\bar{z} - z^*\|_2 + \delta + \epsilon + 2\|\eta\|_2 \right) \\ &= \left( 1 + \frac{C\tilde{K}}{\gamma} \right) \|z^* - \bar{z}\|_2 + \frac{\delta + \epsilon + 2\|\eta\|_2}{\gamma} \end{aligned}$$

□

*Proof of Theorem 4.* Suppose  $\alpha \in (0, 1)$ . By definition of  $A$  and  $B := \begin{bmatrix} A & \sqrt{m}I_m \end{bmatrix}$ , the normalized mixing matrix  $\tilde{B} := m^{-1/2}B$  satisfies S-REC( $F(\mathbb{B}), 1 - \alpha, \delta$ ) with probability at least  $1 - \exp(-cm)$  when

$$m \geq \frac{C\tilde{K}^2}{\alpha^2} \left( k \log \left( \frac{L_G r}{\delta} \right) + k' \log \left( \frac{L_H r'}{\delta} \right) \right).$$

Observe that if  $\lambda := \max\{L_G r, L_H r'\}$  then  $m \geq \frac{C\tilde{K}^2}{\alpha^2} (k + k') \log \left( \frac{\lambda}{\delta} \right)$  implies the above condition. Furthermore, subgaussianity of  $X_z$  gives for any fixed  $z \in \mathbb{R}^n \times \mathbb{R}^m$ ,

$$\left| \|\tilde{B}z\|_2 - \|z\|_2 \right| \leq C\alpha\tilde{K}\|z\|_2$$

with probability at least  $1 - \exp(-\alpha^2 m)$ . Choosing  $\alpha := \frac{1}{2}$  and applying [Lemma 8](#) gives

$$\|\hat{z} - z^*\|_2 \leq C\tilde{K} \min_{z \in F(\mathbb{B})} \|z^* - z\|_2 + C(2\|\eta\|_2 + \delta + \varepsilon).$$

□

## B Proofs for §4

### B.1 Proof of [Lemma 5](#)

It should be noted that the proof of [Lemma 5](#) strongly resembles the proof of an analogous result, [[2](#), Lemma 5]. We include full details here for the sake of clarity to the reader, and note that the proof requires only a handful of changes to leverage an improved Bernstein's inequality, [[12](#), New Bernstein's inequality].

**Theorem** ([[12](#), New Bernstein's inequality]). *Let  $a = (a_1, \dots, a_m)$  be a fixed nonzero vector and let  $Y_1, \dots, Y_m$  be independent, centered subexponential random vectors satisfying  $\mathbb{E}|Y_i| \leq 2$  and  $\|Y_i\|_{\psi_1} \leq K_i^2$  with  $K_i \geq 2$ . Then, for every  $u \geq 0$ ,*

$$\mathbb{P} \left\{ \left| \sum_{i=1}^m a_i Y_i \right| \geq u \right\} \leq 2 \exp \left[ -c \cdot \min \left( \frac{u^2}{\sum_{i=1}^m a_i^2 K_i^2 \log K_i}, \frac{u}{\|a\|_\infty K^2 \log K} \right) \right]$$

where  $K := \max_i K_i$  and  $c$  is an absolute constant.

We will also rely on a version of Hoeffding's inequality for weighted sums of subgaussian random variables. We state this theorem as it appears in [[29](#), Theorem 2.6.3].

**Theorem** ([[29](#), Theorem 2.6.3]). *Let  $X_1, \dots, X_m$  be independent, centered, subgaussian random variables, and  $a = (a_1, \dots, a_m) \in \mathbb{R}^m$ . Then, for every  $t \geq 0$ , we have*

$$\mathbb{P} \left\{ \left| \sum_{i=1}^m a_i X_i \right| \geq t \right\} \leq 2 \exp \left( -\frac{ct^2}{K^2 \|a\|_2^2} \right)$$

where  $K = \max_i \|X_i\|_{\psi_2}$ .

As in the proof of [[2](#), Lemma 5] or [[18](#), Theorem 1.3], we start by proving the result for  $z \in \mathbb{S}^{n+m-1}$  and  $z' = 0$ ; then for  $z, z' \in \mathbb{S}^{n+m-1}$ ; and finally we prove the increment inequality for any  $z, z' \in \mathbb{R}^n \times \mathbb{R}^m$ .

**Lemma 9.** *Suppose  $A \in \mathbb{R}^{m \times n}$  is a  $K$ -subgaussian matrix with  $K \geq 2$ . Then,*

$$\left| \|Ax + \sqrt{m}y\|_2 - \sqrt{m} \right|_{\psi_2} \leq CK\sqrt{\log K}, \quad \text{for every } \begin{bmatrix} x \\ y \end{bmatrix} \in \mathbb{S}^{n+m-1}$$

*Proof of [Lemma 9](#).* For any  $t \geq 0$  we have

$$\begin{aligned} p &:= \mathbb{P} \left\{ \left| \frac{1}{m} \|Ax + \sqrt{m}y\|_2 - 1 \right| \geq t \right\} = \mathbb{P} \left\{ \left| \frac{1}{m} \|Ax\|_2^2 - \|x\|_2^2 + \frac{2}{\sqrt{m}} \langle Ax, y \rangle \right| \geq t \right\} \\ &\leq \mathbb{P} \left\{ \left| \frac{1}{m} \|Ax\|_2^2 - \|x\|_2^2 \right| + \left| \frac{2}{\sqrt{m}} \langle Ax, y \rangle \right| \geq t \right\} \\ &\leq \mathbb{P} \left\{ \left| \frac{1}{m} \|Ax\|_2^2 - \|x\|_2^2 \right| \geq \frac{t}{2} \right\} + \mathbb{P} \left\{ \left| \frac{2}{\sqrt{m}} \langle Ax, y \rangle \right| \geq \frac{t}{2} \right\} =: p_1 + p_2 \end{aligned}$$



To bound  $p_1$ , write

$$\frac{1}{m} \|Ax\|_2^2 - \|x\|_2^2 = \frac{1}{m} \sum [\langle A_i^T, x \rangle^2 - \|x\|_2^2] =: \frac{1}{m} \sum_{i=1}^m Z_i$$

It holds by assumption that the collection  $\{\langle A_i^T, x \rangle\}_{i \in [m]}$  is independent, and that each are centered and subgaussian random vectors with

$$\mathbb{E} \langle A_i^T, x \rangle^2 = \|x\|_2^2 \leq 1 \quad \text{and} \quad \|\langle A_i^T, x \rangle\|_{\psi_2} \leq K \|x\|_2 \leq K.$$

Standard properties of subexponential and subgaussian random variables [29, Chapter 2] thus yield:

$$\|Z_i\|_{\psi_1} = \|\langle A_i^T, x \rangle^2 - \mathbb{E} \langle A_i^T, x \rangle^2\|_{\psi_1} \leq C \|\langle A_i^T, x \rangle^2\| \leq C \|\langle A_i^T, x \rangle\|^2 \leq CK^2.$$

In particular, the assumptions of [12, New Bernstein's inequality] are satisfied. With  $a = (\frac{1}{m}, \dots, \frac{1}{m})$ ,

$$\begin{aligned} p_1 = \mathbb{P} \left\{ \left| \frac{1}{m} \sum_{i=1}^m Z_i \right| \geq \frac{t}{2} \right\} &\leq 2 \exp \left[ -c \cdot \min \left( \frac{mt^2}{CK^2 \log K}, \frac{mt}{CK^2 \log K} \right) \right] \\ &\leq 2 \exp \left[ -\frac{c_1 m}{K^2 \log K} \cdot \min(t^2, t) \right]. \end{aligned}$$

To bound  $p_2$ , we write  $\langle Ax, y_i \rangle = \sum_{i=1}^m y_i \langle A_i^T, x \rangle$  and apply Hoeffding's inequality, noting that  $\|\langle A_i^T, x \rangle\|_{\psi_2} \leq K$ :

$$p_2 = \mathbb{P} \left\{ \left| \frac{1}{\sqrt{m}} \sum_{i=1}^m y_i \langle A_i^T, x \rangle \right| \geq \frac{t}{4} \right\} \leq 2 \exp \left[ -\frac{cmt^2}{K^2 \|y\|_2^2} \right] \leq 2 \exp \left[ -\frac{c_2 mt^2}{K^2 \log K} \right].$$

Here, we have used that  $K \geq 2$  to obtain the right-hand expression. Combining the two bounds gives

$$p \leq 2 \exp \left[ -\frac{c_1 m}{K^2 \log K} \cdot \min(t^2, t) \right] + 2 \exp \left[ -\frac{c_2 mt^2}{K^2 \log K} \right] \leq 4 \exp \left[ -\frac{c_0 m}{K^2 \log K} \min(t^2, t) \right].$$

Next, we establish a concentration inequality for  $\frac{1}{\sqrt{m}} \|Ax + \sqrt{m}y\|_2 - 1$ . Observe that

$$|z - 1| > \delta \implies |z^2 - 1| \geq \max(\delta^2, \delta) \quad \text{for any } z \geq 0, \delta \geq 0.$$

In particular, we set  $t := \max\{\delta^2, \delta\}$  to obtain for any  $\delta \geq 0$ ,

$$\mathbb{P} \left\{ \left| \frac{1}{\sqrt{m}} \|Ax + \sqrt{m}y\|_2 - 1 \right| \geq \delta \right\} \leq \mathbb{P} \left\{ \left| \frac{1}{m} \|Ax + \sqrt{m}y\|_2^2 - 1 \right| \geq \max(\delta^2, \delta) \right\} \leq 4 \exp \left[ -\frac{c_0 m \delta^2}{K^2 \log K} \right].$$

In particular,

$$\left| \left\| Ax + \sqrt{m}y \right\|_2 - \sqrt{m} \right\|_{\psi_2} \leq CK \sqrt{\log K} \quad \text{for any } (x, y) \in \mathbb{S}^{n+m-1}$$

□

**Lemma 10.** Suppose  $A \in \mathbb{R}^{m \times n}$  is a  $K$ -subgaussian matrix with  $K \geq 2$ . Then,

$$\left| \left\| Ax + \sqrt{m}y \right\|_2 - \left\| Ax' + \sqrt{m}y' \right\|_2 \right\|_{\psi_2} \leq CK \sqrt{\log K} \sqrt{\|x - x'\|_2^2 + \|y - y'\|_2^2},$$

for every  $\begin{bmatrix} x \\ y \end{bmatrix}, \begin{bmatrix} x' \\ y' \end{bmatrix} \in \mathbb{S}^{n+m-1}$ .

*Proof of Lemma 10.* It is enough to show that for every  $t \geq 0$

$$p := \mathbb{P} \left\{ \frac{|\|Ax + \sqrt{m}y\|_2 - \|Ax' + \sqrt{m}y'\|_2|}{\sqrt{\|x - x'\|_2^2 + \|y - y'\|_2^2}} \geq t \right\} \leq C \exp \left[ -\frac{ct^2}{K^2 \log K} \right].$$

As in [2, Lemma 7] and [18], we proceed differently for small and large  $t$ .

**First assume** that  $t \geq 2\sqrt{m}$  and let

$$u := \frac{x - x'}{\sqrt{\|x - x'\|_2^2 + \|y - y'\|_2^2}}, \quad v := \frac{y - y'}{\sqrt{\|x - x'\|_2^2 + \|y - y'\|_2^2}}.$$

An application of triangle inequality gives

$$p \leq \mathbb{P} \left\{ \frac{|\|A(x - x') + \sqrt{m}(y - y')\|_2|}{\sqrt{\|x - x'\|_2^2 + \|y - y'\|_2^2}} \geq t \right\} = \mathbb{P} \{ \|Au - \sqrt{m}v\|_2 \geq t \}$$

Subtracting  $\sqrt{m}$  from both sides of the relation describing the event, then using the assumption  $t \geq 2\sqrt{m}$  gives

$$\begin{aligned} \mathbb{P} \{ \|Au - \sqrt{m}v\|_2 \geq t \} &= \mathbb{P} \{ \|Au - \sqrt{m}v\|_2 - \sqrt{m} \geq t - \sqrt{m} \} \\ &\leq \mathbb{P} \left\{ \|Au - \sqrt{m}v\|_2 - \sqrt{m} \geq \frac{t}{2} \right\} \leq 2 \exp \left[ -\frac{ct^2}{K^2 \log K} \right], \end{aligned}$$

where the latter line follows from Lemma 9.

**Next assume** that  $t \leq 2\sqrt{m}$  and define

$$u' := x + x', \quad v' := y + y'.$$

Observe that multiplication by  $\|Ax + \sqrt{m}y\|_2 + \|Ax' + \sqrt{m}y'\|_2$  gives

$$\begin{aligned} p &= \mathbb{P} \left\{ \left| \frac{\|Ax + \sqrt{m}y\|_2^2 - \|Ax' + \sqrt{m}y'\|_2^2}{\sqrt{\|x - x'\|_2^2 + \|y - y'\|_2^2}} \right| \geq t (\|Ax + \sqrt{m}y\|_2 + \|Ax' + \sqrt{m}y'\|_2) \right\} \\ &\leq \mathbb{P} \left\{ \left| \frac{\langle A(x - x') + \sqrt{m}(y - y'), A(x + x') + \sqrt{m}(y + y') \rangle}{\sqrt{\|x - x'\|_2^2 + \|y - y'\|_2^2}} \right| \geq t \cdot \|Ax + \sqrt{m}y\|_2 \right\} \\ &= \mathbb{P} \{ |\langle Au + \sqrt{m}v, Au' + \sqrt{m}v' \rangle| \geq t \cdot \|Ax + \sqrt{m}y\|_2 \}. \end{aligned}$$

Next, define the following events

$$\Omega_0 := \{ |\langle Au + \sqrt{m}v, Au' + \sqrt{m}v' \rangle| \geq t \cdot \|Ax + \sqrt{m}y\|_2 \}, \quad \Omega_1 := \left\{ \|Ax + \sqrt{m}y\|_2 \geq \frac{\sqrt{m}}{2} \right\}.$$

By the law of total probability,

$$\begin{aligned} p &\leq \mathbb{P}(\Omega_0) = \mathbb{P}(\Omega_0 \mid \Omega_1) \cdot \mathbb{P}\{\Omega_1\} + \mathbb{P}(\Omega_0 \mid \Omega_1^C) \cdot \mathbb{P}\{\Omega_1^C\} \\ &\leq \mathbb{P}\{\Omega_0 \mid \Omega_1\} + \mathbb{P}\{\Omega_1^C\} =: p_1 + p_2. \end{aligned}$$

Notice that  $p_2$  may be bounded using Lemma 9. Indeed,

$$\begin{aligned} p_2 &= \mathbb{P} \left\{ \|Ax + \sqrt{m}y\|_2 \leq \frac{\sqrt{m}}{2} \right\} \leq \mathbb{P} \left\{ \left| \|Ax + \sqrt{m}y\|_2 - \sqrt{m} \right| \geq \frac{\sqrt{m}}{2} \right\} \\ &\leq \mathbb{P} \left\{ \left| \|Ax + \sqrt{m}y\|_2 - \sqrt{m} \right| \geq \frac{t}{4} \right\} \leq 2 \exp \left[ -\frac{ct^2}{K^2 \log K} \right]. \end{aligned}$$

Next we bound  $p_1$ . Observe that

$$\begin{aligned}
 p_1 &= \mathbb{P} \{ \Omega_0 \ \& \ \Omega_1 \} \leq \mathbb{P} \left\{ |\langle Au + \sqrt{m}v, Au' + \sqrt{m}v' \rangle| \geq \frac{t\sqrt{m}}{2} \right\} \\
 &\leq \underbrace{\mathbb{P} \left\{ |\langle Au, Au' \rangle + m\langle v, v' \rangle| \geq \frac{t\sqrt{m}}{4} \right\}}_{p_{1a}} \\
 &\quad + \underbrace{\mathbb{P} \left\{ |\sqrt{m}\langle Au, v' \rangle| \geq \frac{t\sqrt{m}}{8} \right\}}_{p_{1b}} + \underbrace{\mathbb{P} \left\{ |\sqrt{m}\langle Au', v \rangle| \geq \frac{t\sqrt{m}}{8} \right\}}_{p_{1c}}.
 \end{aligned}$$

Before we start by bounding  $p_{1a}$ , observe that

$$\langle v, v' \rangle = \frac{\|y\|_2^2 - \|y'\|_2^2}{\sqrt{\|x - x'\|_2^2 + \|y - y'\|_2^2}} = -\frac{\|x\|_2^2 - \|x'\|_2^2}{\sqrt{\|x - x'\|_2^2 + \|y - y'\|_2^2}} = -\langle u, u' \rangle.$$

Consequently,  $p_{1a}$  may be written as

$$\begin{aligned}
 p_{1a} &= \mathbb{P} \left\{ |\langle Au, Au' \rangle + m\langle v, v' \rangle| \geq \frac{t\sqrt{m}}{4} \right\} \\
 &= \mathbb{P} \left\{ |\langle Au, Au' \rangle - m\langle u, u' \rangle| \geq \frac{t\sqrt{m}}{4} \right\} \\
 &= \mathbb{P} \left\{ \left| \sum_{i=1}^m [\langle A_i^T, u \rangle \langle A_i^T, u' \rangle - \langle u, u' \rangle] \right| \geq \frac{t\sqrt{m}}{4} \right\} \\
 &= \mathbb{P} \left\{ \left| \sum_{i=1}^m Z_i \right| \geq \frac{t\sqrt{m}}{4} \right\}.
 \end{aligned}$$

Observe that  $Z_i, i \in [m]$  are independent, centered subexponential random variables satisfying

$$\|Z_i\|_{\psi_1} \leq C\|\langle A_i^T, u \rangle\|_{\psi_2} \cdot C\|\langle A_i^T, u' \rangle\|_{\psi_2} \leq CK^2\|u\|_2\|u'\|_2 \leq CK^2,$$

since  $\|u\|_2, \|u'\|_2 \leq 2$ . Moreover, observe that

$$\begin{aligned}
 \mathbb{E} |Z_i| &= \mathbb{E} |\langle A_i^T, u \rangle \langle A_i^T, u' \rangle - \langle u, u' \rangle| \leq \frac{1}{2} \mathbb{E} [\langle A_i^T, u \rangle^2 + \langle A_i^T, u' \rangle^2] + \langle u, u' \rangle \\
 &= \frac{1}{2} [\|u\|_2^2 + \|u'\|_2^2] + \langle u, u' \rangle = \frac{1}{2} (\|u\|_2 + \|u'\|_2)^2 = \frac{9}{2}.
 \end{aligned}$$

Thus, as per [12, Remark 2.5], there are absolute constants  $c, c' > 0$  such that, by [12, New Bernstein's inequality],

$$p_{1a} \leq 2 \exp \left[ -c' \min \left( \frac{t^2}{16K^2 \log K}, \frac{t\sqrt{m}}{4K^2 \log K} \right) \right] \leq 2 \exp \left[ -\frac{ct^2}{K^2 \log K} \right].$$

Above, the latter inequality follows by  $t \leq 2\sqrt{m}$ . Applying [29, Theorem 2.6.3] bounds  $p_{1b}$  and  $p_{1c}$ :

$$p_{1b} \leq 2 \exp \left[ -\frac{ct^2}{K^2} \right], \quad p_{1c} \leq 2 \exp \left[ -\frac{ct^2}{K^2} \right].$$

Combining  $p_{1a}, p_{1b}, p_{1c}$  and  $p_2$  gives

$$p \leq p_1 + p_2 \leq p_{1a} + p_{1b} + p_{1c} + p_2 \leq C \exp \left[ -\frac{ct^2}{K^2 \log K} \right].$$

□

## B.2 Proof of Theorem 6

*Proof of Lemma 5.* Without loss of generality assume  $\|z\|_2 = 1$  and  $\tau := \|z'\|_2 \geq 1$ . Define  $z'' := x'/\tau$ . Then

$$\|X_z - X_{z'}\|_{\psi_2} \leq \underbrace{\|X_z - X_{z''}\|_{\psi_2}}_{R_1} + \underbrace{\|X_{z''} - X_{z'}\|_{\psi_2}}_{R_2}$$

By Lemma 10,  $R_1 \leq CK\sqrt{\log K}\|z - z''\|_2$ . By collinearity of  $z''$  and  $z'$ , Lemma 9 yields:

$$R_2 = \|X_{z''} - X_{z'}\|_{\psi_2} = \|z' - z''\|_2 \cdot \|X_{z''}\|_{\psi_2} \leq CK\sqrt{\log K} \cdot \|z' - z''\|_2.$$

Combining  $R_1$  and  $R_2$  gives

$$R_1 + R_2 \leq CK\sqrt{\log K}(\|z - z''\|_2 + \|z' - z''\|_2) \leq CK\sqrt{\log K} \cdot \|z - z'\|_2,$$

where the final inequality follows from the “reverse triangle inequality” [29, Exercise 9.1.7]. Accordingly, for any  $z, z' \in \mathbb{R}^n \times \mathbb{R}^m$  one has as desired,

$$\|X_z - X_{z'}\|_{\psi_2} \leq CK\sqrt{\log K} \cdot \|z - z'\|_2.$$

□

*Remark 2.* In Lemma 9 and Lemma 10 it was assumed that  $K \geq 2$ . Notably, any  $K \geq c_0$  for  $c_0 > 1$  would work, leading only to a different value for the absolute constant in the final expression. This bound on  $K$  is necessary to ensure the  $\log K$  term is positive (cf. [12, Remark 2.5]). Fortunately, as noted at the beginning of Subgaussian Lipschitz demixing, the matrices considered in this work admit subgaussian constants satisfying  $K \geq K_0 = (\log 2)^{-1/2} \approx 1.201$ .

## B.2 Proof of Theorem 6

Before proving Theorem 6, we introduce a necessary tool: the majorizing measures theorem.

**Theorem 11** ([18, Theorem 4.1]). *Consider a random process  $(X_z)_{z \in \mathcal{T}}$  indexed by points  $z$  in a bounded set  $\mathcal{T} \subseteq \mathbb{R}^n$ . Assume that the process has sub-gaussian increments: that there exists  $M \geq 0$  such that*

$$\|X_z - X_{z'}\|_{\psi_2} \leq M\|z - z'\|_2 \quad \text{for every } z, z' \in \mathcal{T}.$$

*Then,*

$$\mathbb{E} \sup_{z, z' \in \mathcal{T}} |X_z - X_{z'}| \leq CM \mathbf{w}(\mathcal{T}).$$

*Moreover, for any  $u \geq 0$ , the event*

$$\sup_{z, z' \in \mathcal{T}} |X_z - X_{z'}| \leq CM [\mathbf{w}(\mathcal{T}) + u \cdot \text{diam}(\mathcal{T})]$$

*holds with probability at least  $1 - e^{-u^2}$ , where  $\text{diam}(\mathcal{T}) := \sup_{z, z' \in \mathcal{T}} \|z - z'\|_2$ .*

This phrasing of the theorem appears in [18, Theorem 4.1] and [2, II.B.3] alike. As those authors note, the expectation bound of this theorem can be found in [28, Theorem 2.1.1, 2.1.5]; the high-probability bound in [4, Theorem 3.2].

---

*Proof of Theorem 6.* Combining Lemma 5 and [18, Theorem 4.1] gives, for  $X_z$  as defined in (2),

$$\mathbb{E} \sup_{z, z' \in \mathcal{T}} |X_z - X_{z'}| \leq C\tilde{K} w(\mathcal{T}).$$

Therefore, an application of triangle inequality gives

$$\mathbb{E} \sup_{z \in \mathcal{T}} |X_z| \leq C\tilde{K} w(\mathcal{T}) + \mathbb{E} |X_{z_0}|$$

for some  $z_0 \in \mathcal{T}$  fixed. Applying Lemma 5 to  $\mathcal{T} \cup \{0\}$  gives

$$\mathbb{E} |X_{z_0}| \leq C\tilde{K} \|z_0\|_2.$$

Accordingly, by a standard relation between Gaussian width and complexity (*cf.* Proposition 7),

$$\mathbb{E} \sup_{z \in \mathcal{T}} |X_z| \leq C\tilde{K} w(\mathcal{T}) + \mathbb{E} |X_{z_0}| \leq C\tilde{K} \gamma(\mathcal{T}).$$

An analogous set of steps to those above and in the proof for [2, Theorem 1] yields the high-probability bound.  $\square$

## C Further Numerics Details

In this section we describe the details of the numerical simulations appearing in Numerics. There, two generators were used to run a demixing algorithm supporting the theory developed in Subgaussian Lipschitz demixing. For each generator, a variational autoencoder (VAE) was trained on a set of images and the VAE’s decoder was used as the generator. A pseudo-code meta-algorithm for the numerics is presented in Figure 6. It may serve as a useful roadmap for the steps presented below, though it is at best a terse version of the full description provided in Numerics. We begin by giving a brief overview of VAEs, largely establishing where comprehensive details of our more-or-less standard VAE implementation may be sought.

### C.1 Variational Autoencoders

We provide here some background relevant to our VAE implementation. We claim no novelty of our VAE implementation, noting that a comprehensive overview of our implementation is described in [15, Chapter 2].

The goal of the variational inference problem is to selecting a model  $p_\theta(x)$  with parameters  $\theta$  that approximately models an unknown distribution  $p^*(x)$  over data  $x$ . A common approach introduces a latent variable model with the goal of learning parameters  $\theta$  that capture a joint distribution  $p_\theta(x, z)$  with  $p_\theta(x) = \int p_\theta(x, z) dz \approx p^*(x)$ . Typically, it is intractable to compute the marginal  $p_\theta(x)$  and the posterior distribution  $p_\theta(z | x)$ . Instead, the variational inference approach introduces an *inference model*  $q_\phi(z | x)$  called the *encoder*. The parameters  $\phi$  of the encoder are optimized such that  $q_\phi(z | x) \approx p_\theta(z | x)$ . In the present work, the encoder networks  $\mathcal{E}(x; \phi)$  described above yield parameters  $(\mu, \log(\sigma^2))$  for the distribution  $q_\phi(z | x)$ , which is assumed to be Gaussian. Samples from  $q_\phi$ , then are obtained by “carefully” sampling from a normal distribution. What this means will be described below.

For VAEs, the objective function optimized is the evidence lower bound (ELBO). The ELBO objective (equivalently, ELBO loss) is defined as

$$\mathcal{L}_{\theta, \phi}(x) := \mathbb{E}_{q_\phi(z|x)} [\log p_\theta(x, z) - \log q_\phi(z | x)] = \log p_\theta(x) - D_{KL}(q_\phi(z | x) \parallel p_\theta(z | x)). \quad (11)$$

The ELBO objective (equivalently, ELBO loss) can be efficiently optimized using minibatch SGD and the *reparametrization trick* [15, § 2.4]. Namely, in practice, efficiently computing approximate gradients for minibatch SGD typically makes use of the following steps. The reparametrization trick uses:

$$\begin{aligned}(\mu, \log \sigma^2) &= \mathcal{E}(x; \phi) \\ z &= \mu + \sigma \odot \varepsilon, \quad \varepsilon \sim \mathcal{N}(0, I).\end{aligned}\tag{12}$$

Above,  $\odot$  denotes the element-wise product between its vector arguments. By this computation, the encoder distribution assumes that the latent variables are derived from a Gaussian distribution with diagonal covariance matrix. The parameters of the Gaussian describing the conditional distribution are computed by  $\mathcal{E}(\cdot; \phi)$ . Specifically:

$$\begin{aligned}(\mu, \log \sigma^2) &= \mathcal{E}(x; \phi) \\ q_\phi(z | x) &= \prod_i q_\phi(z_i | x) = \prod_i \mathcal{N}(z_i; \mu_i, \sigma_i^2)\end{aligned}$$

In the present work  $\mathcal{E}(x; \phi)$  is an “encoder” neural network with parameters  $\phi$  and input image  $x \in [0, 1]^{784}$ , with architecture as described in Figure 2a. A VAE acting on an input image  $x$  is thus given by  $A(x) := \mathcal{D} \circ (\mu + \sigma \odot \varepsilon)$  where  $\mu, \sigma, \varepsilon$  are given according to (12),  $\mathcal{D}$  is the decoder network and  $\mathcal{E}$  the encoder network.

The parameters  $\mu, \sigma^2 \in \mathbb{R}^{128}$  are vectors whose elements  $\mu_i, \sigma_i^2$  are the mean and variance corresponding to each of the latent variables  $z_i$ . Note that  $z, \mu, \sigma^2 \in \mathbb{R}^{128}$ , with 128 being the latent dimension, and that these quantities are referred to in Figure 2 by **z**, **mu** and **log\_var**, respectively. In fact, **log\_var** represents the log-variance  $\log \sigma^2$ , which is common to use due to improved numerical stability during training.

In the training of each network, the loss function was the standard implementation used for VAEs. A derivation of the loss function for VAEs in the setting where the encoder is assumed to be Gaussian may be found in [15, Chapter 2.5]. An alternative derivation is given in [21]. We provide an abbreviated description of the loss function here for the sake of completeness. Let  $F$  be a VAE,  $x^{(i)}$  an input image,  $z^{(i)}$  its latent code, and  $x_r^{(i)} = F(X)$  the image reconstructed by the VAE. The loss function in our numerical implementation, expressed for a single datum  $x^{(i)}$ , is given by:

$$\mathcal{L}(x^{(i)}, F) := \text{BCE}(x_r^{(i)}, x^{(i)}) + D_{KL}(q(z | x^{(i)}) \parallel p(z)).$$

The former term is the binary cross-entropy between the image  $x^{(i)}$  and its reconstruction  $x_r^{(i)}$ . The latter term is the KL-divergence between the encoder distribution  $q(z | x^{(i)})$  and the latent prior  $p(z)$ . By construction the latent prior  $p(z)$  is assumed to be standard normal. This loss function may be derived from the general one described in (11). Implementation details for the binary cross-entropy are available in the [PyTorch documentation](#); the KL-divergence in the present setting is equivalent to  $D_{KL}(q_\phi(z_j | x^{(i)}) \parallel p(z)) = \frac{1}{2} [\mu_j^2 + \sigma_j^2 - \log(\sigma_j^2) - 1]$ . Theoretical background and further detail, including on the training of VAEs, is given in [5, 14, 15].

## C.2 Creating the generators

The generators used in these numerical simulations were obtained as the decoders of trained VAEs. The MNIST database [3] of images was used for these simulations. The images of this database are grayscale  $28 \times 28$  images of handwritten digits. Each network only used images corresponding to a single digit class. For this simulation, the digit class 1 was used in training the first VAE, for which there were 7877 images; 8 for the second VAE, for which there were 6825 images. For each network, the images were randomly partitioned into training, validation and test sets (70%, 15%, 15%, respectively). No image augmentations (*e.g.*, random flips or random crops) were used. For both networks, the training batch size was 32, and the number of epochs used for training was

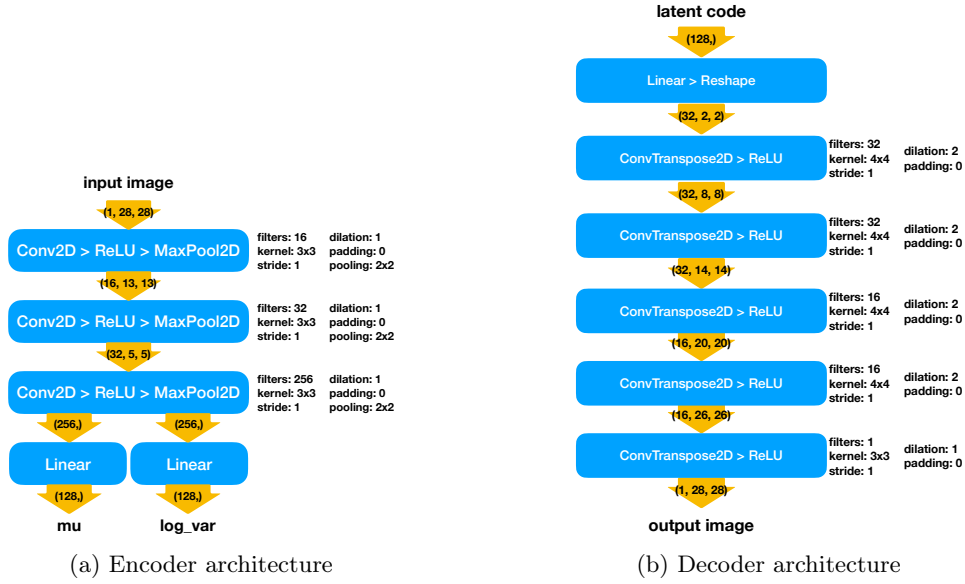


Figure 2: Autoencoder: architecture for the encoder and decoder

200. Early stopping was not used, as we found that the validation loss continued to decrease for the duration of training.

Both networks were variational auto-encoders (VAEs) whose encoders used 2D convolutional layers with max-pooling, and whose decoders used 2D transposed convolutions for image generation. The architectures for the encoder and the decoder are depicted in Figure 2a and 2b, respectively. The latent dimension for both VAEs was 128. Both VAEs assumed that the conditional distribution on the latent codes was Gaussian, as described in Variational Autoencoders. Both VAEs were trained using a modification of mini-batch stochastic gradient descent (SGD) [8] with a learning rate of  $10^{-5}$ , momentum of 0.9 and weight decay of  $10^{-3}$ , using the standard PyTorch implementation of SGD [22]. Results of the training are depicted in Figure 3. In particular, 3a for the VAE trained on 1s, and 3b for the VAE trained on 8s.

Example outputs from noisy latent codes obtained from the validation data are depicted in Figure 4. Specifically, this figure offers a comparison of true images from the validation set and their auto-encoded approximations. Validation images from the 1s dataset can be found in the left panel of Figure 4a, and their reconstructions in the right panel. Validation images from the 8s dataset can be found in the left panel of Figure 4b; their reconstructions in the right panel. The correspondence between the true image and the auto-encoded approximation is given according to the image’s row-column position in the grid.

### C.3 Generative demixing numerical implementation

Generally, the trained encoder network can be interpreted as a map from an image to the encoder’s *latent code* for that image in the VAE’s *latent space*. The decoder can be interpreted as a mapping from the latent space back into the relevant space of natural images. In this way, we are able to use the decoder as a structural proxy corresponding to a low-dimensional representation for an image, just as one might use a particular convex structural proxy like the  $\ell_1$  ball to encode a sparse signal in the classical compressed sensing setting. For further intuition regarding this point we refer the reader to Introduction and [1, 9, 17].

The initial mixture  $b$  for the demixing problem was obtained as described in (3). As a minor technical point, we

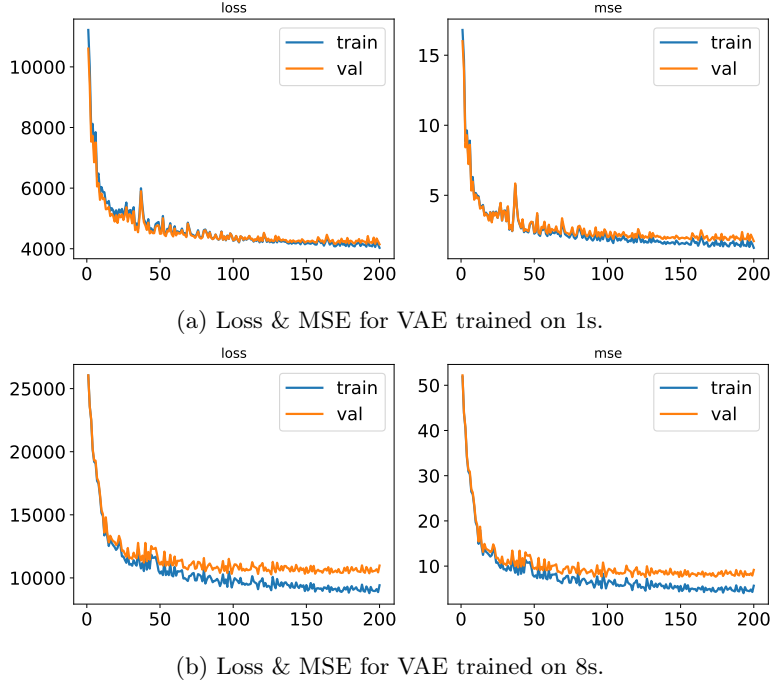


Figure 3: In each sub-figure, the left plot gives the average training and validation loss after each epoch; the right the training and validation MSE after each epoch.

note that the values of the resulting mixture  $b$  were clipped to  $[0, 1]$ , as were those of the predicted mixture at each iteration of the recovery algorithm. We found that the presence of clipping had no apparent effect on recovery performance, but aided visual interpretation of the resulting images. The initial encodings  $w_1^{(0)}, w_8^{(0)} \in \mathbb{R}^{128}$  used by each VAE decoder  $\mathcal{D}_1, \mathcal{D}_8$  were obtained for  $b$  using the VAEs' encoders  $\mathcal{E}_1, \mathcal{E}_8$  and random noise:

$$w_c^{(0)} = \mathcal{E}_c(b) + 0.1 \cdot \varepsilon, \quad c \in \{1, 8\}, \varepsilon_i \stackrel{\text{iid}}{\sim} \mathcal{N}(0, 1).$$

To solve the demixing problem numerically, the MSE loss of the difference between the predicted mixture and the true mixture was minimized using Adam [13] with a learning rate of  $10^{-2}$  for 1000 iterations using PyTorch [22]. Our proposed algorithm, using PyTorch-themed pseudo-code, is presented in Figure 5. For sake of clarity to the reader, we have removed some minor code-specific details, and have used suggestive variable names. The recovered image approximating  $x_1$  had an MSE of  $1.59 \cdot 10^{-3}$ ; that for  $x_8$ ,  $7.48 \cdot 10^{-4}$ ; that for the mixture,  $3.92 \cdot 10^{-4}$ . A graphical depiction of the results appear in Figure 1 as Figures 1a–1h.



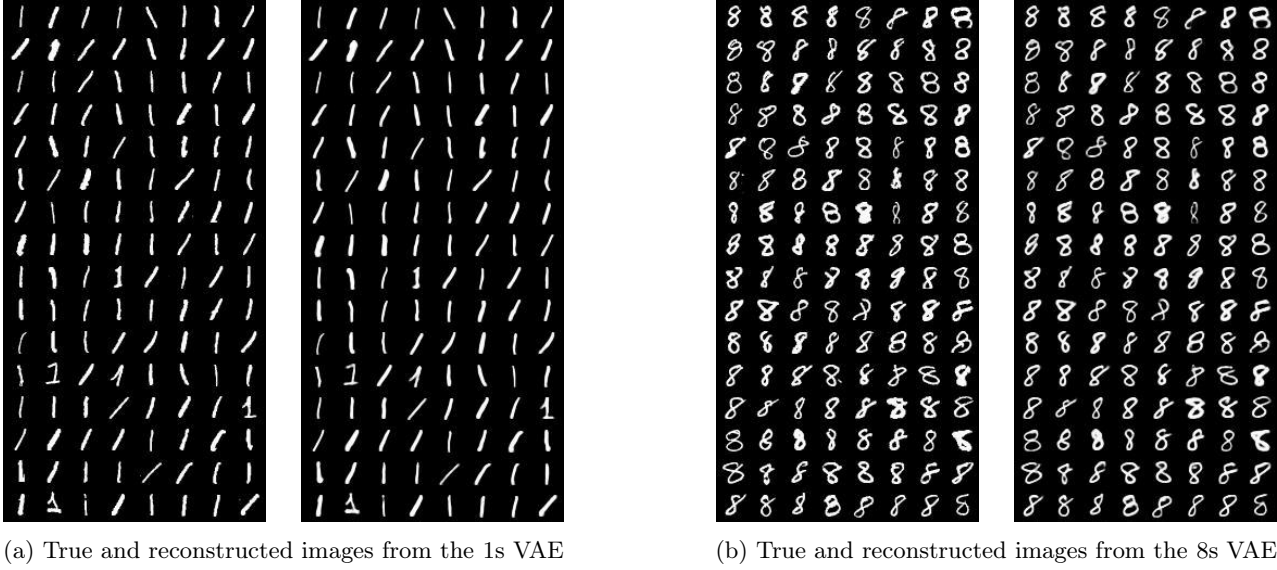


Figure 4: Validation images and their reconstructions by each VAE. In each subfigure, true images from the validation data are shown in the left grid; their reconstruction by the decoder from codes that were partially corrupted are on the right.

```

1  for i in range(num_iter):
2      # compute de-mixed images from latent codes
3      demixed_1 = vae_1.decode(w_1)
4      demixed_8 = vae_8.decode(w_8)
5      # clear gradients from previous iteration
6      optimizer.zero_grad()
7      # obtain predicted mixture
8      mixture_pred = mixer(demixed_1, demixed_8)
9      # compute MSE loss between predicted and true mixture
10     loss = criterion(mixture_pred.view(1, -1), mixture.view(1, -1))
11     # back-propagate to compute gradients
12     loss.backward()
13     # update w_1 and w_8
14     optimizer.step()

```

Figure 5: PyTorch pseudo-code for implementing the demixing algorithm.

```
1 # Establish Architecture
2 Encoder ← GetEncoderArchitecture()
3 Decoder ← GetDecoderArchitecture()
4 AutoEncoder ← function(x, Encoder, Decoder):
5     xReconstructed ← Decoder(SampleFrom(Encoder(x)))
6     Return xReconstructed
7
8 # Train VAEs
9 TrainedDecoder0, TrainedEncoder0 ← MinibatchSGD(
10     Decoder,
11     Encoder,
12     TrainingData0,
13     ValidationData0,
14     VAELoss,
15     VAEOptimizationParameters,
16 )
17 TrainedDecoder1, TrainedEncoder1 ← MinibatchSGD(
18     Decoder,
19     Encoder,
20     TrainingData1,
21     ValidationData1,
22     VAELoss,
23     VAEOptimizationParameters,
24 )
25
26 # Demixing Algorithm
27 x0 ← SampleFrom(TestData0)
28 x1 ← SampleFrom(TestData1)
29 A ← SampleFrom(NormalizedGaussianRandomMatrices)
30 b ← Mult(A, x0) + x1
31 w_init0, w_init1 ← ComputeInitialEncodings()
32 DemixedImage0, DemixedImage1 ← RunDemixing(
33     w_init0,
34     w_init1,
35     TrainedDecoder0,
36     TrainedDecoder1,
37     MSELoss,
38     AdamOptimizer,
39     DemixOptimizationParameters,
40 )
```

Figure 6: A pseudo-code meta-algorithm serving as roadmap for the numerics of this work.